Trans. Phenom. Nano Micro Scales, 7(1): 37-52, Winter and Spring 2019
DOI: 10.22111/tpnms.2018.16247.1098

ORIGINAL RESEARCH PAPER

Numerical analysis of thermal-hydraulic properties of turbulent aerosol-carbon black nanofluid flow in corrugated solar collectors with double application

Ghanbar Ali Sheikhzadeh[1], Farhad Monfaredi[1], Alireza Aghaei[2,], Soroush Sadripour[3], Mohammad Adibi[1]*

[1]*Department of Mechanical Engineering, University of Kashan, Kashan, Iran,*
[2]*Young Researchers and Elite Club, Arak Branch, Islamic Azad University, Arak, Iran*
[3]*Instructor, Faculty of Mechanical Engineering, University of Kashan, Kashan, Iran*

Received 1 August 2016; revised 19 November 2018; accepted 19 November 2018; available online 30 January 2019

ABSTRACT: In this study the effects of corrugated absorber plate and using aerosol-carbon black nanofluid on heat transfer and turbulent flow in solar collectors with double application and air heating collectors, were numerically investigated. The two-dimensional continuity, momentum and energy equation were solved by finite volume and SIMPLE algorithm. In the present investigation all the simulations were done for two different angles of tilt of collector according to horizon, that these angles were the optimum ones for the period of six months setting. As a result the corrugated absorber plate was inspected in the case of triangle, rectangle and sinuous with the wave length of 1 mm and wave amplitude of 3 mm in turbulent flow regime and Reynolds number between 2500 to 4000. Choosing the proper geometry was carried out based on the best performance evaluation criteria (PEC), for collectors with dual usage and increasing the air temperature from collector inlet to outlet for air heating collector. The results revealed that using corrugated absorber plate has a considerable influence on flow field and heat transfer. For all times of the year the highest PEC was obtained for corrugated Sinusoidal model, however the highest temperature increase from inlet to outlet was obtained for rectangular corrugated model. Also it was understood that in the case of using air as a base fluid, whether for the case of temperature increment from inlet to outlet or the highest PEC, the optimum Reynolds is 2500. For each of the corrugated absorber plate with sinusoidal and rectangular models, the carbon black nanoparticles were added to air base fluid in volume fractions of 0.1% to1%. The results indicated that in sinusoidal model the nanoparticles volume fractions increase leads to heat performance coefficient increase and the best heat performance conditions were attained in volume fraction of 1% and Reynolds number of 4000 for both six months period. In rectangular corrugated model using nanofluid and Reynolds number increase do not worth and lead to outlet temperature decrease. Therefore for this model using air and Reynolds number of 2500 is recommended.

KEYWORDS: *corrugated absorber plate; heat performance coefficient; nanofluid Solar collector; performance evaluation criteria; turbulent flow*

INTRODUCTION

The analyses of the international energy organization show that the world energy demand between 2008 and 2035 increases by 35%. According to the limited fossil energy fuels and the side effects of using them on environmental cycle the probe for finding renewable energy in order to deal with this increasing energy demand is necessary. According to international energy agency predictions, more than 13% of this increasing energy demand will be provided by renewable energy [1].

The solar energy is considered as the cleanest, the cheapest and the most accessible energy in the world. The flat plate solar collector comparing with other collector types, has simple design and low costs of construction and in addition to direct solar radiation absorption they can also absorb the emissive radiation [2].

The hot water and air have a wide range of application in industry, agriculture, animal husbandry, and household chor--es. Therefore it is possible to use a collector that can heat water and air at the same time. The present study concentrates on solar collectors with dual usage and solar hot air collectors.

So far lots of numerical and empirical studies related to solar collectors have been conducted. The results of these studies demonstrate that the overall performance of collector is related to many factors including the distance between absorber plate and glass cover and pipe diameter [3-4], wind velocity [5], solar radiation [6], collector material [7], flow rate [8], and channel depth [9].

There are numerous ways to enhance the solar collector efficiency. One way is to use the methods for absorbing more solar radiation.

This method is done by setting the collector angle of tilt and put the collector in the optimized angle of tilt. Khorasanizadeh and Meschi [2] specified the optimized angle of tilt in the case of monthly, seasonally, six months and annual for solar collector in kashan.

*Corresponding Author Email: *A-Aghaei@iau- arak.ac.ir*
Tel.: +989135535460; Note. This manuscript was submitted on August 1, 2016; approved on November 19, 2018; published online January 30, 2019.

Nomenclature

C_k	thermal conductivity ratio
C_μ	turbulence model constant
C_P	specific heat capacity (J/kg.K)
D_h	hydraulic diameter (m)
f	friction factor
G_k	generation rate of TKE
h	heat transfer coefficient ($W/m^2.K$)
H	height of the collector channel (mm)
$\overline{H}$	average of heat flux in 6 months
k	thermal conductivity (W/m.K)
k	turbulent kinetic energy (J/kg)
L	collector length (m)
Nu	Nusselt number
P	pressure (Pa)
Pr	Prandtl number
ΔP	pressure drop (Pa)
PEC	performance evaluation criteria
Q	heat flux
r	sinusoidal geometry function
Re	Reynolds number
t	average of sunny hours in day
T	temperature (K)
u	flow velocity component (m/s)
u′	fluctuated velocity (m/s)

Greek Symbols

α	thermal diffusivity (m^2/s)
α	wavy amplitude (mm)
β	collector slope
Γ	molecular thermal diffusivity
Γ_t	turbulent thermal diffusivity
ε	Turbulent dissipation rate (m^2/s^3)
η	heat performance coefficient
ϑ	kinematic viscosity (m^2/s)
λ	wavelength (cm)
μ	dynamic viscosity (Ns/m^2)
ρ	density (kg/m^3)
ϕ	nanoparticles volume fraction

Subscripts

av	Average
bf	base fluid
c	Local
i, j	components
in	Inlet
nf	Nanofluid
np	nanoparticle
t	Turbulent
w	Wall
0	smooth surface

They suggested of 9° and 51° angle of tilt for setting in the first six months and the second six months, respectively.

The second way is to apply some changes in solar collector geometry in order to reach the highest thermal performance. Getting the heat exchanger jagged and grooved on the interior side is one of the methods for breaking the laminar sub layer and creating the local wall turbulence (due to repetitive flow separation and adhesion between successive grooves). This method decreases the thermal resistance and increases the heat transfer considerably.

Some numerical and experimental researches on the flow fluid and heat transfer inside the corrugated channels have been carried out by some researchers. Comini et al. [10] studied numerically the flow and heat transfer characteristics in three-dimensional wavy channels. They found that the Nusselt number as well as friction factor increases with decreasing aspect ratios. Grant Mills et al [11] conducted a numerical study on heat transfer enhancement and thermal–hydraulic performance in laminar flows through asymmetric wavy wall channels. The results are crucial for designing compact heat exchangers that are capable of having high performance in the laminar regime. Mohamed et al. [12] presented laminar forced convection in the entrance region of a wavy channel. They solved numerically the governing equations using the finite volume method. The effects of Reynolds number, Prandtl number and the amplitude of the corrugation on the flow and thermal fields were introduced by them. It was realized that the shear stresses and Nusselt numbers increase as the Reynolds number increases.Rostami et al [13] investigated optimization of conjugated heat transfer in wavy walls in micro channels. Numerical results reveal that the Nusselt number in wavy microchannels is more than that for flat walls micro channels. Also unlike flat walls microchannels there is an optimum geometry for wavy walls micro channels, which has the maximum Nusselt number. Duan and Muzychka [14] inspected the influences of axial corrugated surface roughness on fully developed laminar flow in micro-tubes analytically. The Stokes equation was solved to predict friction factor and pressure drop in corrugated rough micro-tubes for continuum flow and slip flow. It was observed that there was a significant increase in pressure drop due to roughness.

The third method is to increase the heat transfer between fluid and solar absorbing plate. One common and suggested way is to add the nanoparticles to the base fluid used in collector.

Khoshvaght-Aliabadi [15] analyzed heat transfer and flow characteristics of the sinusoidal-corrugated channels with Al_2O_3-water nanofluid. The effects of different geometrical parameters were calculated at the nanoparticle volume fraction below 4%. The channel height and amplitude indicate the highest influences on Nusselt number and friction factor values. Mohammad et al [16] numerically analyzed the heat transfer and water flow characteristics in a wavy micro channel heat sink (MCHS) and also with different wave amplitude by using the finite volume method.

They found out that the heat transfer coefficient, wall shear stress, pressure drop, and friction factor increase by increasing the wave amplitude through the channel. Heidary and Kermani [17] numerically studied the effect of forced convective heat transfer of Cu-water nanofluid on heat transfer field and flow field in channels with sinusoidal walls. They noticed that by using the nanofluid and horizontal wavy walls at the same time, the heat transfer increases by 50%. Jena and Mahapatra [18] in their numerical modeling investigated the radiative and natural convective heat transfer of aerosol-carbon black nanofluid, in the presence of magnetic field for a two-dimensional chamber. Their results demonstrated that by increasing the volume fraction of carbon black nanoparticles in the base fluid of air, the overall heat transfer inside the chamber will enhance.

Khorasanizadeh et al. [19] investigated the effects of using corrugated absorber plate on heat transfer and turbulent flow in solar air-heater collectors numerically. In their paper choosing the proper geometry was carried out based on the best performance evaluation criteria (PEC) and increasing the air temperature from collector inlet to outlet (ITIO). Their results revealed that using corrugated absorber plate has a considerable influence on flow field and heat transfer. For the whole year the highest PEC was obtained for the sinusoidal corrugated model, however the highest ITIO was obtained for rectangular corrugated model. Also it was known that for the best ITIO and the highest PEC, the optimum Reynolds numbers is 2,500. Sheikhzadeh et al. [20-21], in their papers studied forced turbulent convection flow and heat transfer of air in a desert helicopter cabin. The main aim of their studies was providing human thermal comfort for a desert helicopter pilot in summer (usage of cooling system). In order to fulfill this demand, a body subdomain was considered around the pilot that includes the pilot's using area in cabin by them. The governing equations were numerically solved by the control volume approach based on the SIMPLE technique and standard k-ε turbulent method. The effects of different supply air performances (velocity and temperature) on pilot thermal comfort parameters were presented. Then, the optimization was carried out to reach the optimal case with the minimum predicted percentage dissatisfied (PPD).

Sadripour et al. [22] investigated numerically the thermal comfort parameters and energy saving inside the room with specified dimensions using a ceiling fan with central heating systems during the winter. The flow was turbulent in all models and *k-ε* model was used to simulate turbulence. Rayleigh and Reynolds numbers were in the range of$1.15\times10^{11}\leq Ra\leq 1.55\times10^{11}$ and $6{,}480\leq Re\leq 19{,}440$, respectively. The finite volume method (FVM) and SIMPLE algorithm were used to solve the governing equations. Based on the results, using the ceiling fan during the winter had a considerable effect on improving the thermal comfort and energy saving inside buildings. By using the ceiling fan, the effective room temperature increased by 0.35^{o}C that can be used to reduce the radiators temperature, thereby reducing energy consumption. Additionally, the study results indicated that the location of ceiling fan did not have any effect on room effective temperature and residents' thermal comfort. Sheikhzadeh et al. [23] numerically studied the effects of speed and place of ceiling fans on thermal comfort parameters (PMV and PPD) and energy spending in two different office rooms with certain geometry in winter using district heating system. Based on results, using ceiling fans in winter (heating system) has a considerable influence on improvement of buildings thermal comfort and reducing energy. By using ceiling fans the effective temperature of room increases and therefore radiator energy consumption decreases.

Arani et al. [24] in their paper studied forced convection flow and heat transfer of boehmite alumina in ethylene glycol and water mixture nanofluid in sinusoidal-wavy mini-channel with phase shift and variable wavelength. Their optimization was carried out by using different nanoparticle shapes (spherical, spheroidal, platelets, blades, cylindrical and bricks) to reach the optimal nanoparticle shape with the maximum performance evaluation criterion (PEC). From this study, it is concluded that the thermal-hydraulic performance of channel is greatly influenced by changing the shape of nanoparticles. Using spherical and spheroidal nanoparticles improves the thermal-hydraulic performances of channel, while using non-spherical nanoparticle shapes (platelets, blades, cylindrical and bricks) leads to lower PEC in channel than the base fluid. Sadripour et al. [25] in their study investigated the effects of corrugated absorber plate and using aerosol-carbon black nanofluid on heat transfer and turbulent flow in solar collectors with double application and air heating collectors, numerically. In this investigation all the simulations were done for two different angles of tilt of collector according to horizon, that these angles were the optimum ones for the period of six months setting. As a result the corrugated absorber plate was inspected in the case of triangle, rectangle and sinuous with the wave length of 1mm and wave amplitude of 3mm in turbulent flow regime and Reynolds number between 2,500 to 4,000. Choosing the proper geometry was carried out based on the best performance evaluation criteria (PEC), for collectors with dual usage and increasing the air temperature from collector inlet to outlet for air heating collector. The results revealed that using corrugated absorber plate has a considerable influence on flow field and heat transfer. For all times of the year the highest PEC was obtained for corrugated Sinusoidal model, however the highest temperature increase from inlet to outlet was obtained for rectangular corrugated model. Sadripour [26] studied forced convection flow and heat transfer of MWCNTs-water nanofluid in heat sink collector equipped with mixers. The optimization was carried out by comparison of different parameters to reach the optimal case with the maximum exergy efficiency. From this study, it is concluded that in the case of using heat sink, instead of shell and tubes, the time that the fluid is inside the collector increases and leads to outlet temperature increase from the collector the exergy efficiency increases. Also, it is realized that using mixers enhance the outlet fluid temperature,

energy efficiency and exergy efficiency. Generally, while the trend of exergy efficiency variation with effective parameters is increasing, applying the mixers precipitate the efficiency increment. Sadripour et al. [27] investigated numerically complex heat transfer (turbulent natural convection, conduction and surface thermal radiation) in a rectangular enclosure with a heat source has been carried out. The finite volume method based on SIMPLEC algorithm has been utilized. The effects of Rayleigh number in a range from 10^8 to 10^{11}, internal surface emissivity $0 \leq \varepsilon < 1$ on the fluid flow and heat transfer have been extensively explored. Detailed results including temperature fields, flow profiles, and average Nusselt numbers have been presented. In this investigation it has been tried to study the shape of heat source influence on heat transfer and fluid field in the considered domain. According to results in low emissivity values usage of circular obstacles is recommended. Although in high emissivity values using rectangular obstacles lead to more efficiency.

Sadripour [28] in his study, numerically investigated the effects of corrugated absorber plate and using aerosol/carbon-black nanofluid on heat transfer and turbulent flow in solar collectors. The results revealed that using corrugated absorber plate has a considerable influence on flow field and heat transfer. For all times of the year the highest PEC was obtained for corrugated Sinusoidal model, however the highest temperature increase from inlet to outlet was obtained for rectangular corrugated model. For each of the corrugated absorber plate with sinusoidal and rectangular models, the carbon-black nanoparticles were added to air base fluid in volume fractions of 0.01% to 0.10%. The results indicated that in sinusoidal model the nanoparticles volume fractions increase leads to heat performance coefficient increase and the best heat performance conditions were attained in volume fraction of 0.1% and Reynolds number of 4,000 for both six months period. In rectangular corrugated model using nanofluid and Reynolds number increase do not worth and lead to outlet temperature decrease. In investigation of Sadripour et al. [29], experimental measurements and mathematical modeling are employed to investigate the different parameters, such as temperature of different parts of oven, natural gas consumption, flue gases temperature and portion of different heat transfer mechanisms during baking, in two different traditional flatbread bakeries entitled Sangak (/săngăk/) and Barbari (/bărbări/). In all studied ovens, the bread receives the energy from convection (natural and forced convection), conduction, and radiation (volumetric and surface radiation). The main aim of this study is introduction of a numerical simulation in order to validate and investigate the flatbread bakery ovens. This validation can make the way to analyze different bakery ovens by using numerical methods and consequently reduce the experiments costs. Due to fulfill this demand two numerical models are used and solved using control volume method based on SIMPLE algorithm and RNG k-ε method. The obtained results show that numerical solution can make a reliable result in case of modeling bakery ovens, because of a good agreement between numerical and experimental results with the maximum error of 12.57%. In paper of Sadripour et al. [30], forced convection flow and heat transfer of water in heat sink collector equipped with stationary and rotational obstacles are studied.

The three-dimensional governing equations are numerically solved in the domain by the control volume approach based on the SIMPLE algorithm. Reynolds numbers are considered in laminar-turbulent range of $50 < Re < 12{,}000$. The optimization was carried out by comparison of different parameters to reach the optimal case with the maximum exergy efficiency. From this study, it is concluded that in the case of using heat sink, instead of shell and tubes, the time that the fluid is inside the collector increases and leads to outlet temperature increase from the collector the exergy efficiency increases. Also, it is realized that using the stationary and rotational obstacles enhance the outlet fluid temperature, energy efficiency and exergy efficiency. Nevertheless, using the rotational obstacles is more suitable than using the stationary obstacles. Generally, while the trend of exergy efficiency variation with effective parameters is increasing, applying the obstacles precipitate the efficiency increment. In addition, for the case that the trend of exergy efficiency variation with changing these parameters is decreasing, the decreasing trend gets slow. On the other side, for each special collector there is unique mass flow rate that the exergy efficiency gets maximum value and for higher mass flow rates, primarily the efficiency slightly decreases and then remains unchanged.

Different nanoparticles with various base fluids, higher volume fractions and smaller nanoparticles are found to increase heat transfer [31].

Although in this study the new nanoparticle called carbon black has been used with volume fraction between 0 to 1%. It is inferred from the previous investigations that no numerical studies has been carried out on aerosol-carbon black nanofluid with turbulent flow inside the solar collector with corrugated walls.

In lots of aforementioned numerical investigations the effects of corrugated plates on enhancing heat transfer in channels have been done and the comparison between smooth and sinusoidal corrugated channels has been made. However for solar collectors, the accurate comparison between linear corrugated models (rectangular and triangular) and nonlinear models (sinusoidal) has not been made in the case of Nusselt number, pressure drop, friction factor, PEC, and the difference between inlet and outlet temperature, and mainly the considered collectors were solar flat plate collectors.

In current investigation the precise comparison for scrutinizing the thermal-hydraulic characteristics of the turbulent air flow and aerosol-carbon black nanofluid inside collectors with rectangular, triangular, and sinusoidal corrugated absorbing plate has been made by numerical procedure. Among absorbing plates with different corrugations, the optimized configurations have been chosen based on the higher PEC and difference between inlet and

outlet temperature. Then the effects of aerosol-carbon black nanofluid on the thermal-hydraulic characteristics and temperature increase from inlet to outlet are analyzed for these optimized configurations.

NUMERICAL MODELING

Physical Model

The schematic diagram of the two-dimensional collector with entrance height of $2H$=20mm is shown in Figure 1.

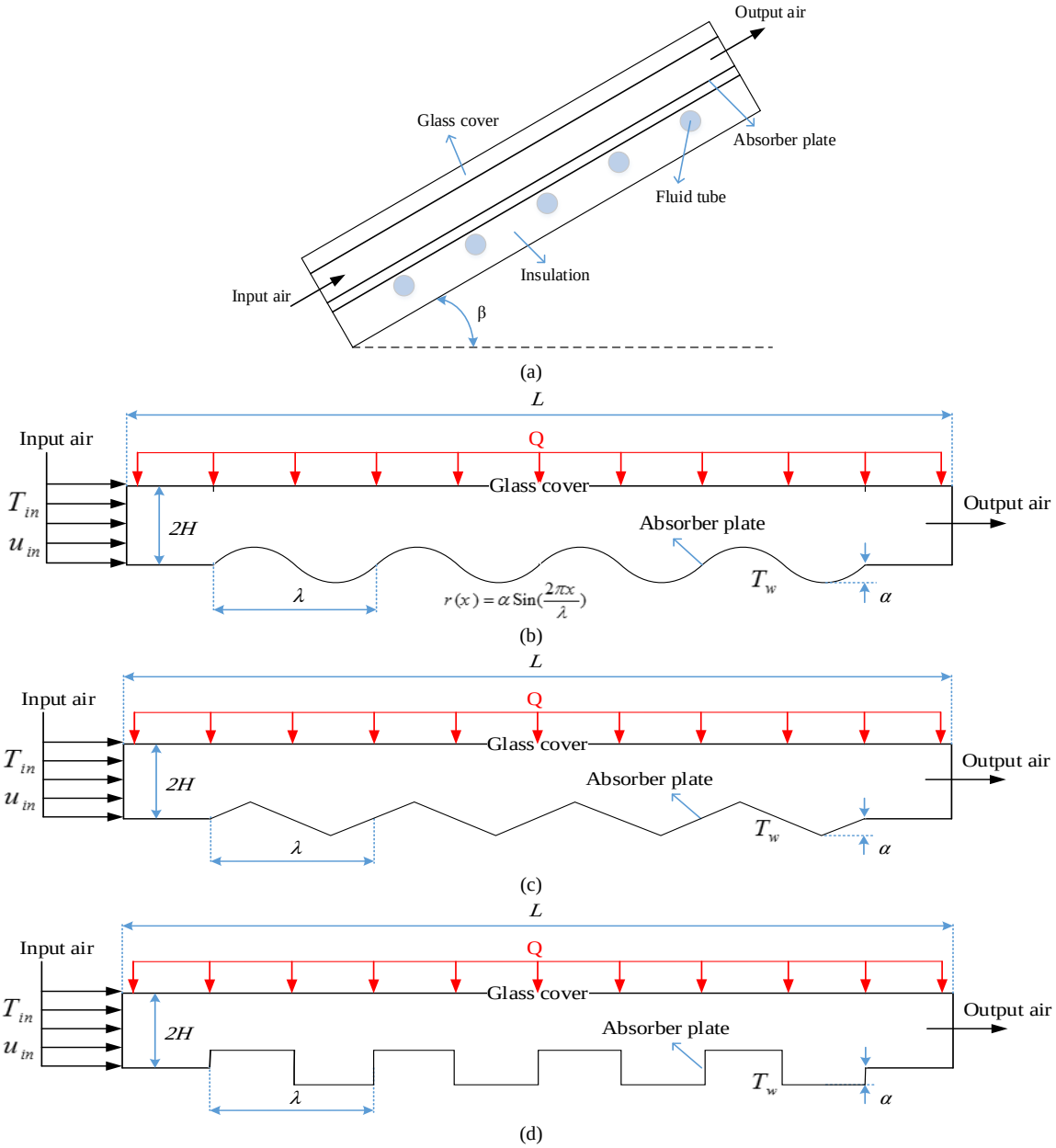

Fig. 1. (a) The schematic diagram of the two dimensional collector with double application. Two dimensional solar collector models with: (b) sinusoidal corrugation, (c) triangular corrugation, and (d) rectangular corrugation. (The actual geometry consists of 18 corrugations but for clear presentation only 4 waves have been shown.)

The problem geometry includes two-dimensional corrugated walls with 18 waves along the length of the test-section. The heat transfer and flow field are studied for sinusoidal, triangular and rectangular corrugations. The wave length of the walls in all three models is $\lambda = 1$ cm and the wave amplitude is $\alpha = 3$ mm. The collector length equals to $L = 2$ m. For the left section of the channel the velocity inlet boundary condition in Reynolds number between 2500 and 4000 is considered and for the outlet section of the channel pressure outlet boundary condition is assumed. The absorber plate is in the constant and uniform temperature. This temperature has been obtained by the

empirical measurements for the installed collectors in Kashan with 51° longitude and 30 minutes in east direction and 34° latitude and 5 minute in north direction located in Iran for the first and second period of the year. The glass cover has the constant heat flux boundary condition that the inlet heat flux value for the first and second period of the year is obtained from[2]. The flow inside the channel is considered steady and turbulent. The ambient temperature for the both periods of the year is different too and these data are collected from Iran's weather forecast organization for Kashan[32].

Governing Equations

In this section the governing equations related to heat transfer and flow field are presented [33]. The considerations are as follows:

1. Steady state and two-dimensional.
2. Incompressible flow.
3. The flow properties are independent of the temperature.

Continuity equation

$$\frac{\partial}{\partial x_i}(\rho u_i) = 0 \tag{1}$$

where ρ is the density and u_i is the axial velocity.

Momentum equation

$$\frac{\partial}{\partial x_j}(\rho u_i u_j) = -\frac{\partial P}{\partial x_i} + \frac{\partial}{\partial x_j} \left[\mu\left(\frac{\partial u_i}{\partial x_j} + \frac{\partial u_j}{\partial x_i}\right)\right] + \frac{\partial}{\partial x_j}(-\rho\overline{u_i' u_j'}) \tag{2}$$

In the above equationμ andu' are fluid viscosity and fluctuated velocity, respectively. The term of$\rho\overline{u_i' u_j'}$ indicates the Reynolds stress.

Energy equation

$$\frac{\partial}{\partial x_i}(\rho u_i T) = \frac{\partial}{\partial x_j}\left[(\Gamma + \Gamma_t)\frac{\partial T}{\partial x_j}\right] \tag{3}$$

where Γ and Γ_t are the molecular thermal diffusivity and turbulent thermal diffusivity, respectively and are defined as follow:

$$\Gamma = \frac{\mu}{\mathrm{Pr}} \text{ and } \Gamma_t = \frac{\mu_t}{\mathrm{Pr}_t} \tag{4}$$

In order to model the turbulence it is necessary to model the Reynolds stress in equation 3. The standard k-ε model has been used for turbulence modeling. One common way to connect the Reynolds stress to average velocity gradients is Bossinisque assumption.

$$\left(-\rho\overline{u_i' u_j'}\right) = \mu_t\left(\frac{\partial u_i}{\partial x_j} + \frac{\partial u_j}{\partial x_i}\right) \tag{5}$$

The turbulent viscosity is derived from equation 6:

$$\mu_t = \rho C_\mu \frac{k^2}{\varepsilon} \tag{6}$$

The kinetic energy conservation equation and the loss rate are measured from equation 7 and 8:

$$\frac{\partial}{\partial x_i}[\rho k u_i] = \frac{\partial}{\partial x_j}\left[\left(\mu + \frac{\mu_t}{\sigma_k}\right)\frac{\partial k}{\partial x_j}\right] + G_k - \rho\varepsilon \tag{7}$$

$$\frac{\partial}{\partial x_i}[\rho\varepsilon u_i] = \frac{\partial}{\partial x_j}\left[\left(\mu + \frac{\mu_t}{\sigma_\varepsilon}\right)\frac{\partial \varepsilon}{\partial x_j}\right] + C_{1\varepsilon}\frac{\varepsilon}{k}G_k + C_{2\varepsilon}\rho\frac{\varepsilon^2}{k} \tag{8}$$

where G_k is the turbulent kinetic energy generation rate and $\rho\varepsilon$ is the loss rate and is defined by:

$$G_k = -\rho\overline{u_i' u_j'}\frac{\partial u_j}{\partial x_i} \tag{9}$$

The boundary values for turbulence adjacent to the wall are specified by enhanced wall treatment. The coefficients$C_\mu = 0.09$, $C_{1\varepsilon} = 1.44$, $C_{2\varepsilon} = 1.92$, $\sigma_k = 1.0$, $\sigma_\varepsilon = 1.3$ and $Pr_t = 0.85$ are chosen as empirical coefficients in turbulence transport equation [34]. The Nusselt number, Reynolds number, friction factor, performance evaluation criteria and heat performance coefficient are non-dimensional parameters that are calculated from the below equations [17, 35]:

$$Nu_{av} = \frac{h_f D_h}{k_f} \tag{10}$$

In the above equation h and k are conducting heat transfer coefficient and convective heat transfer coefficient respectively.

In the present work the Nusselt number is measured on the absorber plate.

$$Re = \frac{\rho_f u_{in} D_h}{\mu_f} \tag{11}$$

In this equation u_{in} is the average velocity of the fluid in the collector inlet.

The hydraulic diameter is also defined as follows:

$$D_h = 2H + \alpha \tag{12}$$

$$f = \frac{2}{\left(\frac{L}{D_h}\right)} \frac{\Delta P}{\rho_{nf} {u_{in}}^2} \tag{13}$$

where ΔP is the pressure difference between collector inlet and outlet.

$$\Delta P = P_{av,inlet} - P_{av,outlet} \tag{14}$$

Where $P_{av,inlet}$ and $P_{av,outlet}$ are average pressure in inlet and outlet, respectively.

In order to compare the effect of Nusselt number change to pressure drop with corrugated absorber plate usage toward smooth absorber plate the performance evaluation criteria (PEC) is calculated by the below equation 36:

$$PEC = \left(\frac{Nu}{Nu_0}\right) \cdot \left(\frac{f}{f_0}\right)^{-1/3} \tag{15}$$

In the above equation Nu and Nu_0 are average Nusselt number in corrugated collector and average Nusselt number in collector with smooth absorber plate, respectively. On the other hand f and f_0 are friction factor inside the corrugated collector and collector with smooth absorber plate respectively.

Equation 16 is used to compare the effect of using the nanofluid on average Nusselt number and pressure drop toward base fluid usage [37]:

$$\eta = \left(\frac{Nu_{nf}}{Nu_f}\right) \cdot \left(\frac{f_{nf}}{f_f}\right)^{-1/3} \tag{16}$$

Where Nu_{nf} and f_{nf} are average Nusselt number and friction factor in collector with nanofluid, respectively and Nu_f and f_f are average Nusselt number and friction factor in collector with fluid, respectively.

The temperature difference from inlet to outlet is computed by:

$$\Delta T = T_{av,outlet} - T_{av,inlet} \tag{17}$$

Where $T_{av,outlet}$ and $T_{av,inlet}$ are average temperature in inlet and outlet.

Thermal diffusion coefficient, kinematic viscosity and prantdl number for fluid and nanofluid are calculated from the below equations:

$$\alpha = \frac{k}{\rho\, C_p} \tag{18}$$

$$\vartheta = \frac{\mu}{\rho} \tag{19}$$

$$Pr = \frac{\vartheta}{\alpha} \tag{20}$$

The local Nusselt number in the isothermal wall is measured by [18]:

$$Nu_c = -\left(\frac{k_{nf}}{k_f}\right)\frac{\partial T}{\partial y} \tag{21}$$

In the above equation $\frac{\partial T}{\partial y}$ is the temperature gradient in thermal boundary layer.

MODEL VALIDATION

Grid Independence Test

The grid independence test was done for collector with air fluid.

According to Figure 2, four different grids with 143476, 145327, 149771 and 151825 nodes are considered for the smooth absorber plate model.

By comparing the four cases the grid with 149771 nodes is chosen as an acceptable grid.

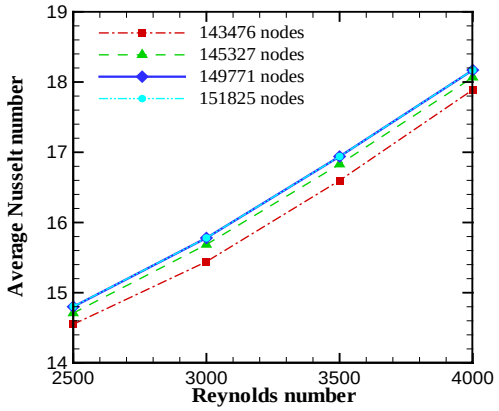

Fig. 2. Average Nusselt number variation diagram according to Reynolds number for different grid sizes in smooth absorber plate

Validation

The computer software validation was done based on the geometry and boundary condition of [36].

In this study the heat transfer performance and water flow forced convective heat transfer in a heated channel with corrugated wall is investigated.

The average Nusselt number and friction factor are compared in Figure 3.

It is clear that there is a good conformity between the results.

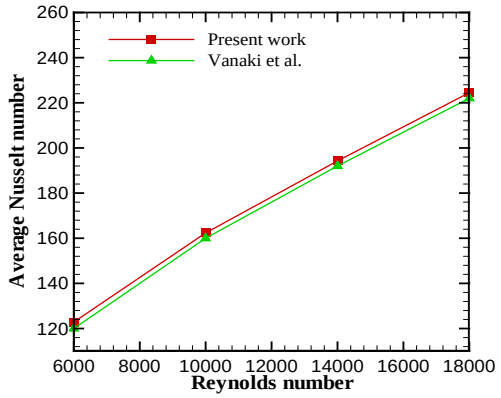

(a)

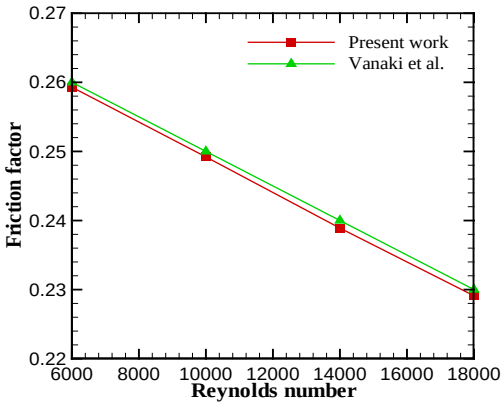

(b)

Fig. 3. Current research validation for a) average Nusselt number, b) friction coefficient, in comparison with [36] in a sinusoidal corrugated channel with phase shift of 180° and amplitude of 1 mm

Thermophysical Properties of Nanofluid

The nanofluid density and specific heat transfer in a reference temperature T_{in} is shown with ρ_{nf} and $(C_p)_{nf}$ respectively [18]:

$$\rho_{nf} = (1-\phi)\rho_{bf} + \phi\rho_{np} \tag{22}$$

$$(\rho C_p)_{nf} = (1-\phi)(\rho C_p)_f + \phi(\rho C_p)_s \tag{23}$$

The carbon black nanoparticles in nanofluid mixture are considered spherical and the thermal conductivity is computed by [18]:

$$\frac{k_{nf}}{k_f} = \frac{k_s + 2k_f - 2\phi(k_f - k_s)}{k_s + 2k_f + \phi(k_f - k_s)} \tag{24}$$

The nanofluid viscosity is calculated by [38]:

$$\mu_{nf} = \frac{\mu_f}{(1-\phi)^{2.5}} \tag{25}$$

The thermo physical properties of carbon black nanoparticles and air are listed in Table 1.

Table 1
Effect of spatial resolution on the mean Nusselt number at different Rayleigh numbers.

Thermophysical properties	Air	Carbon Black
$\rho(Kg/m^3)$	1.225	2000
$C_p(J/Kg\cdot K)$	1006.43	710
$k\ (W/m\cdot K)$	0.0242	2000
$\mu(Ns/m^2)$	0.000017894	-

Numerical Procedure

A steady numerical simulation from the flow field was considered through the two-dimensional corrugated channel to solv and investigate the flow and heat transfer model. The control volume method and SIMPLE algorithm were applied to solve the equations.

The turbulent standard k-ε model was used with enhanced wall treatment.

The numerical calculation was carried out by solving the governing equations with boundary conditions and with finite volume method.

The diffusion term in momentum and energy equations and for convective term were discretisized by the second order backward difference. The error value was 10^{-5} in order all parameters converge.

Boundary Conditions and Environmental Properties

The average daily temperature of Kashan for the first and second period of the year is 297 K and 282 K, respectively. These data are collected from the average temperature for the first and second period of the year based on the Iran's weather forecast organization [32].

The ambient pressure for Kashan is 88588 Pa [2] and the gravity acceleration is 9.806. The heat flux on the glass cover is computed by:

$$Q = \frac{\bar{H}}{3600\ t} \tag{26}$$

In this equation $\bar{H}$ is the six months average for daily flux on horizontal surface and t is the average sunny hours during the day. The glass transmission coefficient is 0.88 and absorption coefficient for aluminum with dark cover is 0.95 [39].

Because this work is based on the six months setting of the flat plate collector, the average sunny hours, average daily temperature, and monthly average of daily flux from sun on the horizontal surface must be calculated in Kashan for the first and second six months period.

Therefore with using equation 26 the received flux amount by glass cover is obtained for the first and second six months period. In addition the empirical calculation of absorber plate temperature during the year for Kashan shows that the average temperature of absorber plate for this city is approximately constant for a specified period of time. The results of these measurements are presented in Table 2.

Table 2

The average sunny hours, average daily temperature, monthly average daily flux received from sun on the horizontal surface for Kashan, the received flux by glass cover and absorber plate temperature during the first and second six months of the year.

Period of time	Average sunny hours during the day	Average daily temperature	Monthly average daily heat flux on horizon surface $\bar{H}$	Received heat flux by glass cover	Absorber plate temperature
	(hr)	(K)	(MJ/m^2.day)	(W/m^2)	(K)
Spring and Summer	10.25	297	25.35	687	355
Fall and Winter	7.6	282	13.87	507	345

RESULTS AND DISCUSSION

In this section the effects of using the corrugated absorber plate for different Reynolds number on flow and heat transfer field are inspected.

Also the effects of the carbon black nanoparticle are studied.

Whether the optimized thermal-hydraulic performance is of high interest or outlet temperature increase, the appropriate shape of corrugations is chosen. adopting the appropriate corrugation shape for optimized thermal-hydraulic performance is based on equation 15 and for the highest air temperature in outlet is based on equation 17. Then for the optimized corrugation shape the effect of using nanofluid on flow and heat transfer is investigated.

The Effect of Corrugation Shape of the Absorber plate on Thermal-Hydraulic Characteristics

In this section the effect of using corrugated absorber plate with different shapes on the flow and heat transfer is analyzed for the first and second six months period. In Figures 4a and 5a, the diagram of average Nusselt number change according to Reynolds number for the first and second six months period is shown, respectively.

It is observed that by increasing the Reynolds number, the average Nusselt number increases too. In fact higher Reynolds numbers indicate higher velocities that lead to turbulent flow and therefore enhance the heat transfer. The results reveal that the average Nusselt numbers for corrugated absorber plate are always higher than the smooth plate.

This is due to more turbulence and consequently thinner boundary layer in corrugated channels that causes higher temperature gradients.

The triangular corrugated channels in the first and second six months of the year have the highest average Nusselt number in all Reynolds number and also they can intensify the heat transfer to 27% and 25% in comparison with smooth channels in Reynolds numbers equal to 2500 for the first and second six months of the year, respectively. Furthermore comparing to smooth channels, the corrugated absorber plate with sinusoidal shape can increase the heat transfer to 25% and 23% in Reynolds number of 2500, for the first and seco-nd six months of the year, respectively.

Figures 4d and 5b show PEC according to Reynolds number.

The PEC values have decreasing and similar behavior for all models in the first and second six months of the year within investigated Reynolds number and for the mentioned collectors PEC decreases by increasing the Reynolds number.

As it is seen in figure 4although Nusselt number increases by increasing the Reynolds number, the pressure drop is also increasing.

However increasing the Nusselt number cannot conquer the growth of pressure drop and finally it leads to PEC decrease by increasing Reynolds number.

Therefore for the maximum value of the PEC it is possible to determine the optimized Reynolds number for each absorber shape. The optimized Reynolds number for all models is 2500.

The collector with sinusoidal absorber plate has the best PEC among all configurations that is 1.08 and 1.06 for first and second six months of the year, respectively.

Figures 4c and 5c show the diagram of temperature increase variation from inlet to outlet in the range of mentioned Reynolds number for the first and second six months of the year.

It is observed that the temperature increase in corrugated collectors is more than the smooth collectors in all corrugated models during both periods.

Among these collectors the rectangular corrugated collectors during the first and second six months have more temperature increase from inlet to outlet and after that the sinusoidal and triangular corrugated collectors are ranked, respectively.

The highest value of temperature increase in the low Reynolds range for the rectangular corrugated was about 63 K for the first six months and 59 K for the second six months these values for the sinusoidal and triangular models were 59 K and 55 K, respectively while these values were 53 K for the first and 48 K for the second six months of the year in smooth collectors.

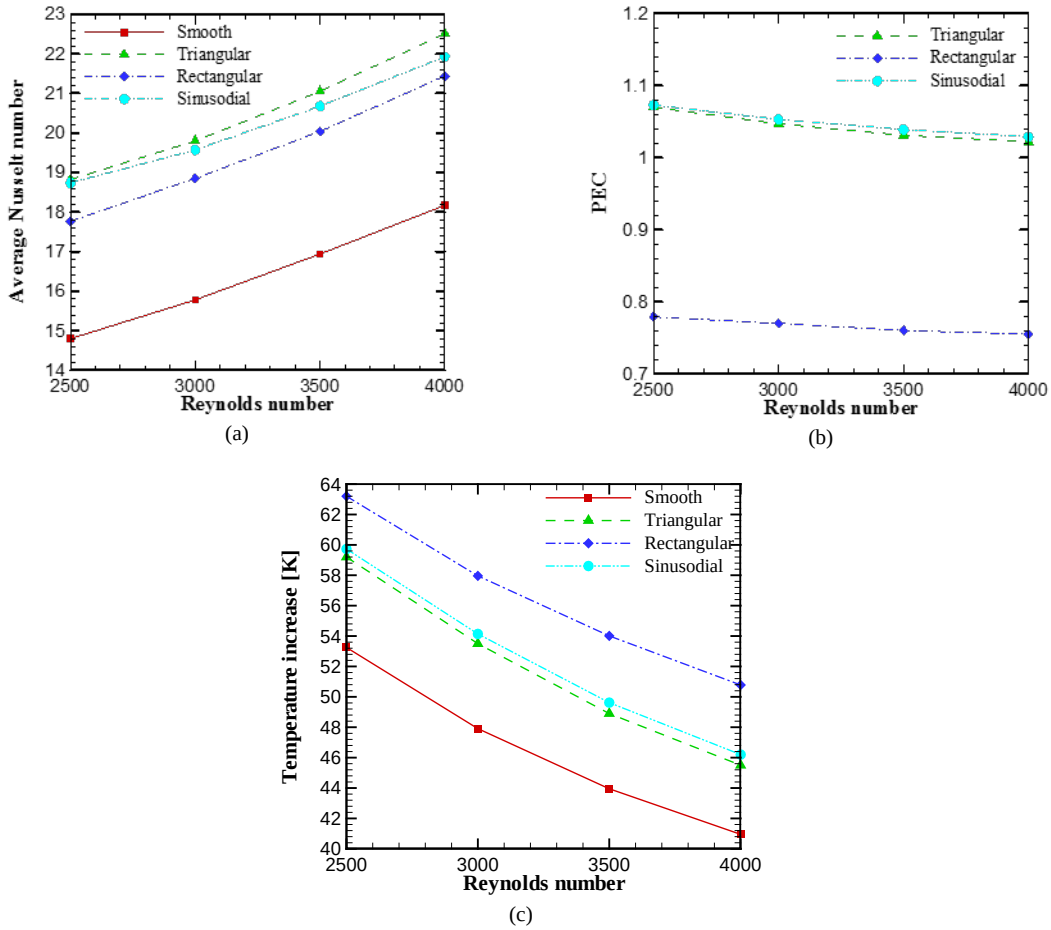

Fig. 4. Variation diagram of (a) average Nusselt number, (b) PEC, (c) air temperature increment from collector inlet to outlet, according to different Reynolds number for corrugated and smooth absorber plates during the first six months

According to the aforementioned discussion the sinusoidal corrugated model is chosen as an optimized model in case of thermal-hydraulic performance due to highest PEC.

However in the case of pressure drop it is the best model and overall by considering these two parameters together it was chosen as the most appropriate model for the conditions that heat is needed to be transferred to installed pipes under the absorber plate and also by the optimized performance of the pumping system with the least losses,the air temperature increases, throughout the year.

On the other hand for the condition that the solar collector is supposed to be used increasing the air temperature and the pumping system performance and losses are not important, the rectangular corrugated model was adopted because it has the most temperature increase among all models.

The Effect of Using NanoFluid in Different Volume Fractions

In this part the effect of using the aerosol-carbon black nanofluid with spherical nanoparticle and different volume fractions on flow and heat transfer field of rectangular and sinusoidal corrugations is investigated.

Figures 6 and 7 show the diagram of non-dimensional thermo physical properties change for aerosol- carbon black nanofluid in different volume fractions of carbon black nanoparticles.

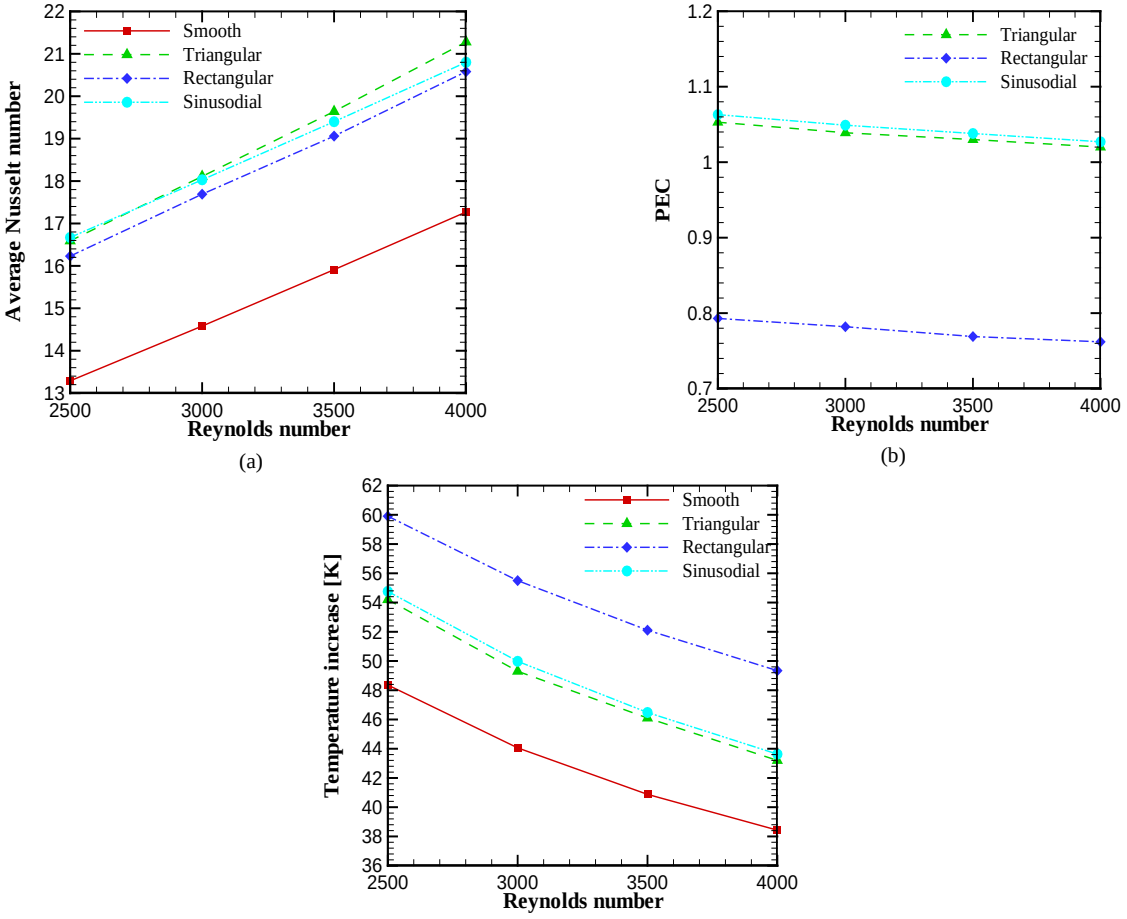

Fig. 5. Variation diagram of (a) average Nusselt number, (b) PEC, (c) air temperature increment from collector inlet to outlet, according to different Reynolds number for corrugated and smooth absorber plates during the second six months

As can be seen in Figure 6 by increasing volume fraction of carbon black nanoparticle from 0 to 1% the thermal conductivity and dynamic viscosity of nanofluid according to base fluid do not have the intense variation and ultimately each of them increases to 3% and 2.5%, respectively.

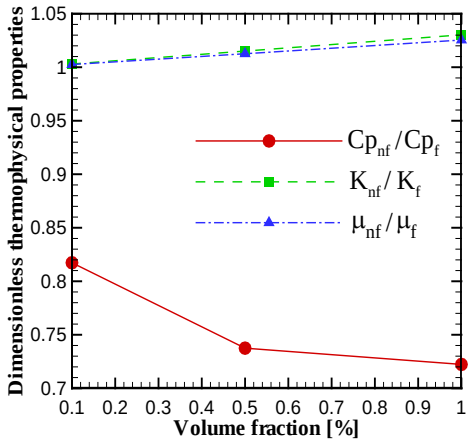

Fig. 6. Non-dimensional specific heat, thermal conductivity and dynamic viscosity according to carbon black nanoparticle volume fraction in nanofluid mixture

But as can be seen the nanofluid specific heat variation compared to base fluid has an intense changes and it increases to 28%. In contrast it is observed in Figure 7 that the nanofluid density in volume fraction of 1% to 17.5% increases like base fluid density.

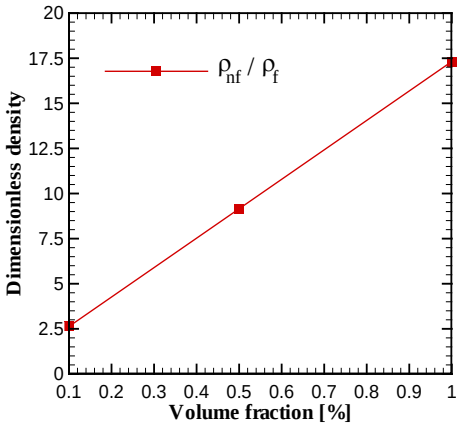

Fig. 7. Non-dimensional density variation according to carbon black nanoparticle volume fraction in nanofluid mixture

As can be seen in Figures 8a and 9a by increasing the volume fraction of carbon black nanoparticles in air, the average Nusselt number increases as well inside the collector with sinusoidal absorber plate for the first and second six months of the year. As it is observed in the figure for example in Reynolds number of 4000 with volume fraction of 1% the Nusselt number increases by 455% and 483% for the first and second months of the year, respectively.

It was perceived that in the Figure 6 nanofluid thermal conductivity increase is not much comparing to the base fluid so it is not possible to attribute this increase in Nusselt number to thermal conductivity however it has an impact on Nusselt number increase certainly.

But as it was seen the nanofluid density and specific heat have great changes comparing base fluid. The calculation with equations of 18 to 20 showed that the Prandtl number is approximately 0.74415 in the case of using the base fluid this demonstrates that the thermal boundary layer thickness is more than velocity boundary layer. By increasing the volume fraction of carbon black nanoparticles the Prandtle number decreased and for instance it reached to 0.53497 in volume fraction of 1%.

Besides in the case of using nanofluid the thermal diffusion coefficient and kinetic viscosity decrease were noticed while the kinetic viscosity decrease was more intense.

These items show that in the case of using nanofluid the thermal and velocity boundary layers become thinner.

The intense increase in thermal boundary layer based on equation 21 leads to temperature gradient increase within thermal boundary layer and consequently the Nusselt number increases on the absorber surface as well as nanofluid thermal conductivity.

By increasing the nanoparticles volume fraction and Reynolds number the static pressure drop increases from inlet to outlet in collector.

The reason for increasing the static pressure drop with nanoparticle volume fraction increase is the nanofluid density and viscosity increment.

In addition by increasing the nanofluid volume fraction the friction factor decreases. The reason for this is more intense growth in nanofluid dynamic pressure according to static pressure drop because the nanofluid density is significantly increasing.

Figures 8b and 9b show the heat performance coefficient diagram in the case of using nanofluid in different volume fractions and for various Reynolds numbers in a collector with sinusoidal absorber plate during the first and second six months of the year, respectively.

As it is seen the heat performance coefficient increases by increasing Reynolds number.

This is due to increasing the Nusselt number and decreasing friction factor with Reynolds number increment. Furthermore by increasing the volume fraction, heat performance coefficient increases too. The reason for this is similar increase in the Nusselt number and decrease in the friction factor by Nusselt number increment. Consequently in the case of using sinusoidal absorber plate with aerosol-carbon black nanofluid, the highest heat performance coefficient was obtained in Reynolds 4000 and volume fraction of 1% for both first and second six months of year.

Figures 8c and 9c show the diagram of temperature increase changes from collector inlet to outlet in the range of discussed Reynolds numbers for different nanofluid volume fractions inside the collector with sinusoidal absorber plate during the first and second six months of the year.

It is observed that for all volume fractions during both periods of time the temperature increment inside the collector having nanofluid is less than the collector having the base fluid.

In the volume fraction of 1% during both periods of time the least temperature increase was observed from inlet to outlet and after that the volume fractions of 0.5% and 0.1% were like that respectively.

The least temperature increment in low Reynolds numbers was 20 K for the first six months of the year and 22 K for the second six months of the year in the volume fraction of 1% and these values were 40 K and 38 K for the volume fraction of 0.1% respectively.

While for the collector having the base fluid these amounts were 50 K for the first six months of the year and 54 K for the second six months of the year.

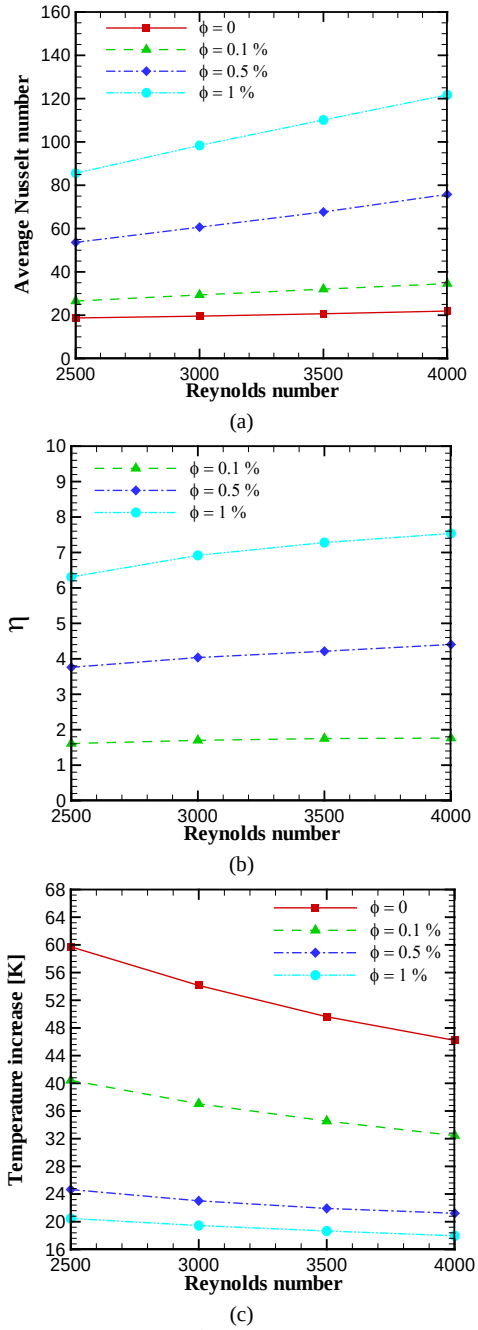

Fig. 8. Variation diagram of (a) average Nusselt number, (b) heat performance coefficient, (c) air temperature increment from collector inlet to outlet, according to different Reynolds number for sinusoidal corrugated absorber in various nanoparticle volume fractions during the first six months of the year

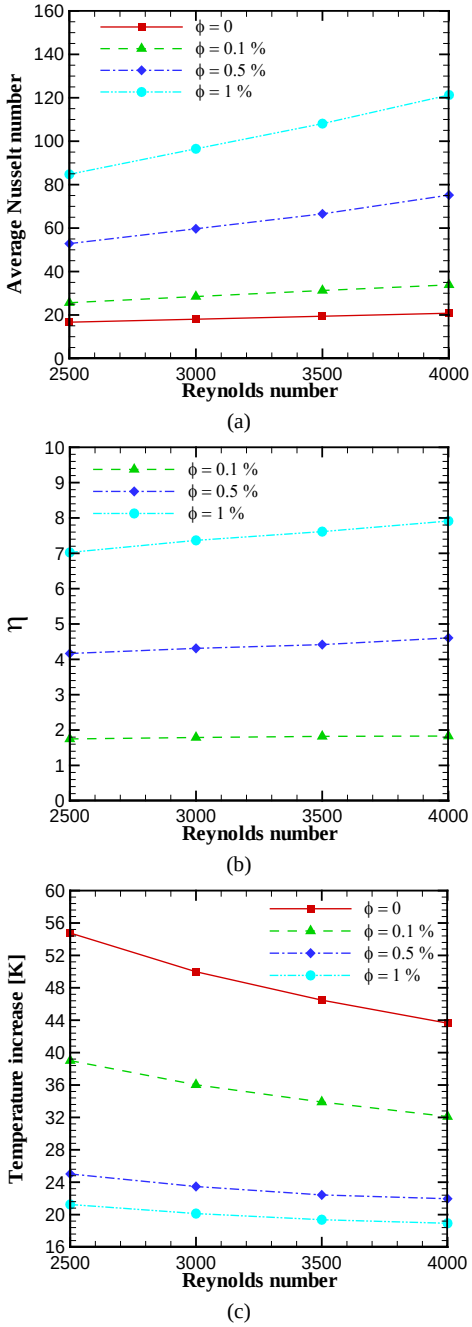

Fig. 9. Variation diagram of (a) average Nusselt number, (b) heat performance coefficient, (c) air temperature increment from collector inlet to outlet, according to different Reynolds number for sinusoidal corrugated absorber in various nanoparticle volume fractions during the second six months of the year

As a result if the temperature increase from inlet to outlet is only considered for the collector with sinusoidal absorber plate the nanofluid usage will not be recommended because it substantially decreases the temperature increment from inlet to outlet. In addition it is proposed to use the collector in low Reynolds number since by increasing the fluid velocity the temperature increment from inlet to outlet decreases throughout the year.

As can be noted in Figure 10a and 11a by increasing the volume fraction of carbon black nanoparticles in air, the average Nusselt number increases too inside the collector with rectangular absorber plate for the first and second six months of the year.

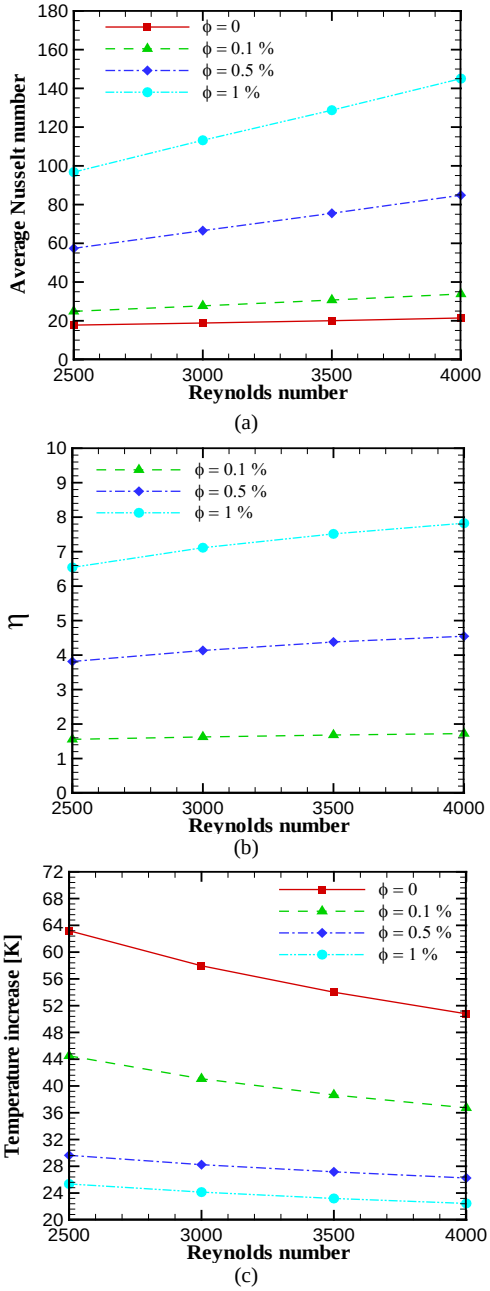

Fig. 10. Variation diagram of (a) average Nusselt number, (b) heat performance coefficient, (c) air temperature increment from collector inlet to outlet, according to different Reynolds number for rectangular corrugated absorber in various volume fractions during the first six months of the year.

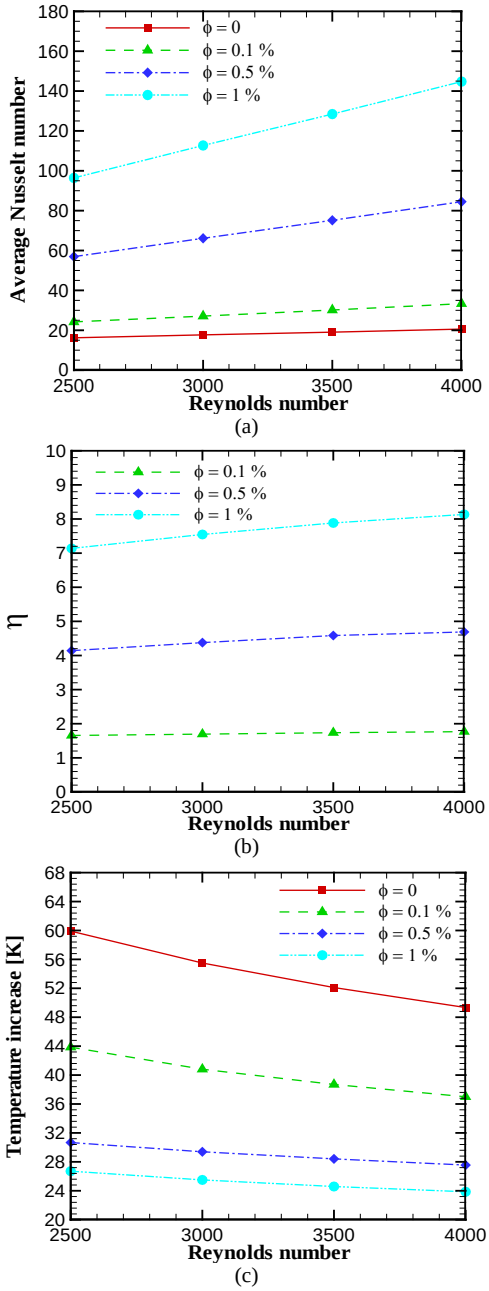

Fig. 11. Variation diagram of (a) average Nusselt number, (b) heat performance coefficient, (c) air temperature increment from collector inlet to outlet, according to different Reynolds number for rectangular corrugated absorber in various volume fractions during the second six months of the year

Based on Figures 10b and 11b by increasing the Reynolds number and volume fraction the ηvalue increases. Therefore it was found out that in the case of using the rectangular absorber plate with aerosol-carbon black nanofluid the highest thermal performance coefficient is obtained in the Reynolds of 4000 and volume fraction of 1% during the first and second six months of the year.

Figures 10c and 11c show the diagram of temperature increase variation from collector inlet to outlet in the range of discussed Reynolds numbers for different nanofluid volume fractions inside the collector with rectangular absorber plate during the first and second six months of the year. It is seen that in all volume fractions during both periods of time, the temperature increment in a collector that has a nanofluid is less than the collector with the base fluid. In the volume fraction of 1% during both periods of time the

least temperature increase was observed from inlet to outlet and after that the volume fractions of 0.5% and 0.1% were ranked, respectively. The least temperature increment in low Reynolds numbers for volume fraction of 1% was 25 K during the first six months and it was 26 during the second six months and these values were approximately 44 K for volume fraction of 0.1%. Hence in case of using the model with rectangular corrugated absorber plate, if fluid temperature increment from inlet to outlet is only considered, the nanofluid usage will not be recommended because it considerably decreases the temperature increase from inlet to outlet. Moreover it is advised to use the collector in low Reynolds numbers due to the temperature increase from collector inlet to outlet decreases by velocity increment in all cases throughout the year.

CONCLUSION

A numerical study was carried out in order to investigate the thermal-hydraulic behaviors of air forced convective heat transfer inside the collector with dual usage and corrugated absorber plate for turbulent regime in the range of turbulent Reynolds numbers between 2500 and 4000. The solar collector with dual usage means a collector that is able to transfer the heatto the fluid inside the installed pipes under the absorber plate and also the heat transfer to the air passing between the absorber plate and glass cover. The focus of the present study has been on enhancing the heat transfer because of corrugated absorber plate by breaking the laminar sub-layer and producing local wall turbulence due to flow separation and adherence between successive grooves again that decreases the thermal resistance and intensifies the heat transfer considerably. As stated by the results corrugating the absorber plate improves the thermal characteristics like Nusselt number and temperature increment from inlet to outlet but in the case of hydraulic characteristics it enhances the losses. For this reason by defining the PEC that is a compromised point between improving the heat transfer characteristics andpressure drop compensation, it is possible to obtain the optimized model. On that account the results indicate that despite this fact that the collectors with triangular and rectangular absorber plate have the highest Nusselt number as well as highest temperature increase from inlet to outlet throughout the year respectively due to friction factor increase and pressure drop compensation but since the collector with sinusoidal absorber plate has the highest PEC for the whole year, the corrugated sinusoidal model is introduced as the optimized model in the current study. On the other hand if the air temperature increase is only considered the rectangular corrugated model is the optimized one. The results revealed that in the case of using the air base fluid whether in term of temperature increase from inlet to outlet or in term of the highest PEC,the optimized Reynolds number is 2500. For each of the sinusoidal and rectangular corrugated models throughout the year the carbon black nanoparticles were added to the air base fluid in the volume fractions of 0.1% to 1%. The results showed that in sinusoidal model which is used because of transferring more heat to the fluid inside the pipes installed under the absorber plate and also the outlet air temperature increase between the absorber plate and glass cover, the nanoparticle volume fraction increase leads to thermal performance coefficient increment and in Reynolds number of 4000 and volume fraction of 1% the optimized model was obtained for the whole year. In rectangular corrugated model that is simulated to increase the air temperature only the nanofluid usage and Reynolds number increment are not useful at all and lead to outlet temperature decrease. So for this model the base fluid usage and 2500 Reynolds number are recommended.

REFERENCES

[1] Organisation for Economic Co-operation and Development/International Energy Association, World Energy, Outlook 2011, 2011.

[2] Khorasanizadeh H, Meschi M. Determination of the monthly, seasonal, semi-yearly and yearly optimum tilt angles of flat plate solar collectors in Kashan. Journal of Energy Engineering Management. 2014; 3 (4): 38-49.

[3] Leon M A, Kumar S. Mathematical modeling and thermal performance analysis of unglazed transpired solar collectors. Sol. Energy. 2007; 81: 62–75.

[4] Motahar S, Alemrajabi A.A. An analysis of unglazed transpired solar collectors based on exergetic performance criteria, Int. J. Thermodyn. 2010; 13 (4): 153–160.

[5] Kutscher C F, Christensen C B, Barker G M. Unglazed transpired solar collectors: heat loss theory, J. Sol. Energy Eng. 1993; 115: 182–188.

[6] Yildiz C, Torgrul I.T, Sarsilmaz C, Pehlivan D. Thermal efficiency of an air solar collector with extended absorption surface and increased convection, Int. Commun. Heat Mass Transfer. 2002; 29 (6): 831–840.

[7] Tsilingiris P T. Heat transfer analysis of low thermal conductivity solar energy absorbers, Appl. Therm. Eng. 2000; 20: 1297–1314.

[8] Khattab N M, Evaluation of perforated plate solar air heater, Int. J. Sol. Energy. 2000; 21: 45–62.

[9] Njomo D, Daguenet M. Sensitivity analysis of thermal performances of flat plate solar air heaters, Heat Mass Transfer. 2006; 42: 1065–1081.

[10] Comini G, Nonino C, Savino S. Effect of aspect ratio on convection enhancement in wavy channels, Numerical Heat Transfer. Part A. 2003; 44: 21-37.

[11] Grant Mills Z, Warey A, Alexeev A. Heat transfer enhancement and thermal–hydraulic performance in laminar flows through asymmetric wavy walled channels, International Journal of Heat and Mass Transfer. 2016; 97: 450–460.

[12] Mohamed N, Khedidja B, Belkacem Z, Michel D. Numerical study of laminar forced convection in entrance region of a wavy channel, Numerical Heat Transfer, Part A. 2008; 53: 35-52.

[13] Rostami J, Abbassi A, Saffar-Avval M. Optimization of conjugate heat transfer in wavy walls microchannels, Applied Thermal Engineering. 2015; 82: 318-328.

[14] Duan Z, Muzychka Y S. Effects of axial corrugated roughness on low Reynolds number slip flow and continuum flow in micro-tubes, Journal of Heat Transfer. 2010; 132: 1–8.

[15] Khoshvaght-Aliabadi M. Influence of different design parameters and Al2O3 water nanofluid flow on heat transfer and flow characteristics of sinusoidal corrugated channels, Energy Conversation and Management. 2014; 88: 96–105.

[16] Mohammed H A, Gunnasegaran P, Shuaib N H. Numerical simulation of heat transfer enhancement in wavy microchannel heat sink, Int. Commun. Heat Mass Transfer. 2011; 38: 63-72.

[17] Heidary H, Kermani M. Effect of nano-particles on forced convection in sinusoidal-wall channel, International Communications in Heat and Mass Transfer. 2010; 37: 1520-1527.

[18] Jena S K, Mahapatra, S K. Numerical modeling of interaction between surface radiation and natural convection of atmospheric aerosol in presence of transverse magnetic field, Applied Mathemathical Modeling. 2013; 37: 527-539

[19] Khorasanizadeh H, Sadripour S, Aghaei A. Numerical investigation of thermo-hydraulic characteristics of corrugated air-heater solar collectors. Modares Mechanical Engineering. 2016; 16 (13): 42-46, (In Persian).

[20] Sheikhzadeh Gh A, Sadripour S, Aghaei A, Shahrezaee M B. An investigation of human thermal comfort in a desert helicopter, Conference International Conference on air conditioning and heating / cooling installations. 2016; 2: 78-86.

[21] Sheikhzadeh Gh A, Sadripour S, Aghaei A, Shahrezaee M B, Babaei M R. Providing human thermal comfort conditions for pilot in a desert helicopter. Modares Mechanical Engineering. 2016; 16 (13): 100-103, (In Persian).

[22] Sadripour S, Mollamahdi M, Sheikhzadeh Gh A, Adibi M. Providing thermal comfort and saving energy inside the buildings using a ceiling fan in heating systems. Journal of the Brazilian Society of Mechanical Sciences and Engineering. 2017; 39 (10), 4219-4239.

[23] Sheikhzadeh Gh A, Sadripour S, Mollamahdi M. Numerical study of effect of speed and place of ceiling fans on thermal comfort and reducing energy in office buildings. Amirkabir Journal of Mechanical Engineering. 2018; 50 (2): 309-326.

[24] Abbasian Arani A A, Sadripour S, Kermani S. Nanoparticle shape effects on thermal-hydraulic performance of boehmite alumina nanofluids in a sinusoidal–wavy mini-channel with phase shift and variable wavelength. International Journal of Mechanical Sciences. 2017; 128–129: 550–563,.

[25] Sadripour S, Adibi M, Sheikhzadeh Gh A. Two different viewpoints about using aerosol-carbon nanofluid in corrugated solar collectors: Thermal-hydraulic performance, and heating performance. Global Journal of Researches in Engineering A: Mechanical and Mechanics. 2017; 17(5): 37–48.

[26] Sadripour S. First and second laws analysis and optimization of a solar absorber; using insulator mixers and MWCNTs nanoparticles. Global Journal of Researches in Engineering A: Mechanical and Mechanics. 2017; 17(5): 37–48.

[27] Sadripour S, Ghorashi S A, Estajloo M. Numerical Investigation of a Corrugated Heat Source Cavity: A Full Convection-Conduction-Radiation Coupling. American Journal of Aerospace Engineering. 2017; 4(3): 27-37.

[28] Sadripour S. 3D Numerical Analysis of Atmospheric-Aerosol/Carbon-Black Nanofluid Flow within a Solar Air Heater Located in Shiraz, Iran. International Journal of Numerical Methods for Heat and Fluid Flow, The article is published in Early Cite section of journal. https://www.emeraldinsight.com/doi/full/10.1108/HFF-04-2018-0169.

[29] Sadripour S, Estajloo M, Hashemi S A, Adibi M. Experimental and Numerical Investigation of Two Different Traditional Hand-Baking Flatbread Bakery Units Located in Kashan, Iran. International Journal of Engineering Transactions B: Applications. 2018; 31 (8): 1292–1301.

[30] Sadripour S, Abbasian Arani A A, Kermani S. Energy and Exergy Analysis and Optimization of a Heat Sink Collector Equipped with Rotational Obstacles. AUT Journal of Mechanical Engineering. 2018; 2 (1): 39–50.

[31] Mohammed H A, Al-Shamani A N, Sheriff J M. Thermal and hydraulic characteristics of turbulent nanofluids flow in a rib–groove channel, Int. Commun. Heat Mass Transfer. 2012; 39: 158-164.

[32] Meteorological Organization I.R. Of Iran, http://www.irimo.ir

[33] Eiamsa-ard S, Promvonge P. Numerical study on heat transfer of turbulent channel flow over periodic grooves, International Communications in Heat and Mass Transfer. 2008; 35: 844-852.

[34] Launder BE, Spalding DB. Mathematical models of turbulence. Academic press; 1972.

[35] Mohammed H A, Abbas A K, Sheriff J M. Influence of geometrical parameters and forced convective heat transfer in transversely corrugated circular tubes, Int. Commun. Heat Mass Transfer. 2013; 44: 116-126.

[36] Vanaki Sh M, Mohammed H A, Abdollahi A, Wahid M A. Effect of nanoparticle shapes on the heat transfer enhancement in a wavy channel with different phase shifts. Journal of Molecular Liquids. 2014; 196: 32-42.

[37] Karwa R, Sharma Ch, Karwa N. Performance Evaluation Criterion at Equal Pumping Power for Enhanced Performance Heat Transfer Surfaces. 2013; Hindawi.

[38] Brinkman H.C. The viscosity of concentrated suspensions and solutions, J. Chem. Phys. 1952; 20: 571–581.

[39] Duffie JA, Beckman WA. Solar engineering of thermal processes. John Wiley & Sons; 2013 Apr 15.